Journal of Mammalian Evolution
https://doi.org/10.1007/s10914-020-09502-z

REVIEW

Integration or Modularity in the Mandible of Canids (Carnivora: Canidae): a Geometric Morphometric Approach

Valentina Segura[1,2] · Guillermo H. Cassini[2,3,4] · Francisco J. Prevosti[2,5] · Fabio Andrade Machado[2,3,6]

Abstract

Understanding the interplay between morphological integration and modularity is considered an important topic in the study of the evolution of the form of complex structures. The mandible is a complex structure that can be shaped by diverse factors such as ontogeny, ecology, and evolutionary history. In canids, this is particularly interesting because they have a large diversity in feeding behavior and hunting strategy. Here, we employed geometric morphometric techniques to evaluate the balance between integration and modularity in 1011 mandibles of a sample of extinct and extant canids. The results show that allometric scaling seems to have little influence in determining the mandibular shape of canids. Some divergence associated with ecology was observed, especially for highly specialized taxa (hypercarnivores and insectivores). Finally, macroevolutionary patterns were more integrated than intraspecific patterns, suggesting that correlational selection might play a strong role in the evolution of mandibular form and function. We found no evidence of an evolutionary line of least resistance in shaping mandible disparity.

Keywords Carnivora · Canidae · Mandible · Integration · Modularity

Introduction

Organisms are integrated wholes that are constituted of multiple semi-independent anatomical structures, or modules, that might arise from different embryological pathways, functioning independently of one another and having independent evolutionary histories (Klingenberg et al. 2004; Klingenberg 2008). The degree of covariation between these parts relates to concepts of morphological integration and modularity (Klingenberg 2009). Morphological integration is the coordinated variation of these different parts (Olson and Miller 1958; Cheverud 1996), while modularity refers to the formation of modules, which are internally cohesive units marked by the strong interconnection among their parts and, relative independence from other modules (Klingenberg et al. 2004; Esteve-Altava 2017). This not only means that modules are thought to be able to be modified without interfering with others (Garcia et al. 2014), but also that more modular organisms are capable of more finely adapting the various aspects of their morphology to diverging selective pressures (Curth et al.

Electronic supplementary material The online version of this article (https://doi.org/10.1007/s10914-020-09502-z) contains supplementary material, which is available to authorized users.

✉ Valentina Segura
vseguragago@gmail.com

[1] Unidad Ejecutora Lillo, Consejo Nacional de Investigaciones Científicas y Técnicas–Fundación Miguel Lillo, Miguel Lillo 251, 4000 San Miguel de Tucumán, Argentina

[2] Consejo Nacional de Investigaciones Científicas y Técnicas (CONICET), Buenos Aires, Argentina

[3] División Mastozoología, Museo Argentino de Ciencias Naturales "Bernardino Rivadavia", Av. Ángel Gallardo 470, C1405DJR Ciudad Autónoma de Buenos Aires, Argentina

[4] Departamento de Ciencias Básicas, Universidad Nacional de Luján, Ruta 5 y Av. Constitución s/n, Luján, 6700 Buenos Aires, Argentina

[5] Museo de Ciencias Antropológicas y Naturales, Universidad Nacional de La Rioja (UNLaR), Av. Luis M. de la Fuente s/n, 5300 La Rioja, Argentina

[6] Department of Biology, University of Massachusetts, 100 William T. Morrissey Blvd, Boston, MA 02125, USA

Published online: 30 April 2020

2017; Larouche et al. 2018). On the other hand, a strong integration may act as a constraint and influence the direction of evolution (Hansen and Houle 2008; Parr et al. 2016). For this reason, understanding the interplay between integration and modularity is considered an important topic in the study of the evolution of the form of complex structures (Hallgrímsson et al. 2009; Parr et al. 2016); such is the case of the mandible of mammals.

The mammalian mandible originates from cranial neural crest cells that migrate to the first pharyngeal arch and generate a ventral condensation. From this condensation, Meckel's cartilage develops and gives rise to the mandible (Cerny et al. 2004). The mandible is a structure that plays a key role in catching and handling prey and in mastication (Wainwright and Reilly 1994). These functions are related with two mandibular units: the alveolar region and the ascending ramus, which respectively bear teeth and provide attachment for masticatory muscles such as the masseter, temporalis, and pterygoids (Meloro et al. 2008; Meloro and O'Higgins 2011). While both units are developmentally distinct and relate to different orofacial systems, they are also connected by the need to perform an integrated function defined by the species ecology. Thus, the contrast between development and ecology is no more evident than in this structure, raising the question of which of those two factors is more effective in determining the evolution of mandibular form.

Here, we investigate this issue in the Canidae family (Carnivora). Canids are very diverse in their feeding behavior and strategy (Ewer 1998; Slater et al. 2009), posing an ideal evolutionary system for the investigation of the effect of ecology on morphology. In fact, there is a wealth of evidence pointing to the fact that mandible morphology is influenced by ecology (Radinsky 1981a, 1981b; Biknevicius and Ruff 1992; Holliday and Steppan 2004; Meloro et al. 2008; Tseng and Binder 2009; La Croix et al. 2011a, 2011b; Prevosti et al. 2011; Meloro and O'Higgins 2011; Echarri and Prevosti 2015), suggesting a major role of function in the determination of form. While studies of intraspecific variation and modularity of the canid mandible are generally scarce (e.g., Prevosti et al. 2013), canids are thought to have a more modular skull than other carnivorans (Machado et al. 2018), with facial traits varying more independently. This skull modularity might translate into the variation of the mandible, as a variation in facial length would most likely affect the alveolar region, but not necessarily the ascending ramus, potentially making this system ideal to dissect the interplay between those contradictory forces.

In this study, we employ geometric morphometrics techniques to evaluate the balance between integration and modularity in the mandible of a sample of extinct and extant canids. We investigate patterns of morphological evolution and the relative influence of allometry, phylogeny, and integration in constraining the change within the lineage. Additionally, we confront the patterns of between-species divergence with intraspecific constraints to evaluate the relative effect of modularity in facilitating the evolution of the structure. The match between intra- and interspecific patterns of variation is usually interpreted as the presence of lines of evolutionary least resistance (LLR) where genetic and ontogenetic factors facilitate evolutionary change along some directions of the morphospace and constrains it along others (Schluter 1996). It has recently been suggested that the mandible of Canidae evolved along a LLR that is similar to that followed by Mustelidae and Felidae (Conith et al. 2018). However this inference was based exclusively on macroevolutionary patterns and did not investigate the action of within-species constraints. Here, we test this prediction, and discuss our findings in terms of the ecology and function of the structure in the group and its consequences in the study of morphological constraints.

Materials and Methods

Sample

The sample consisted of 1011 mandibles of adult canids of the 19 extant and two extinct species (Fig. 1). The majority of our sample is concentrated on the South American canids (Cerdocyonia sensu Zrzavý et al. 2018), both in terms of intraspecific and interspecific variation. Our sample of the clade Canina and of the grade Vulpini (sensu Zrzavý et al. 2018) covers both basal and derived taxa, covering large portions of the form disparity within the group. The material studied belongs to the mammal collections of the AMNH (American Museum of Natural History, New York, USA), CFA (Colección Félix de Azara, Buenos Aires, Argentina), CML (Colección Mamíferos Lillo, Tucumán, Argentina), FMNH (Field Museum of Natural History, Chicago, USA), GECM (Colección Grupo de Ecología Comportamental de Mamíferos, Bahía Blanca, Argentina), LIEB (Colección de Mamíferos del Laboratorio de Investigaciones en Evolución y Biodiversidad, Esquel, Argentina), MACN (Museo Argentino de Ciencias Naturales Bernardino Rivadavia, Buenos Aires, Argentina), MFAZV (Museo Florentino Ameghino de Zoología de vertebrados, Santa Fe, Argentina), MLP (Museo de La Plata, La Plata, Argentina), MZUSP (Museu de zoología da Universidade de São Paulo, São Paulo, Brazil), and NMNH (National Museum of Natural History, Washington, D.C., USA) (Appendix 1).

Landmarks

Eighteen landmarks were digitized in three dimensions with a Microscribe MX6DOF System (GoMeasured3D, Amherst, VA, USA). These landmarks were types 1, 2, and 3 sensu

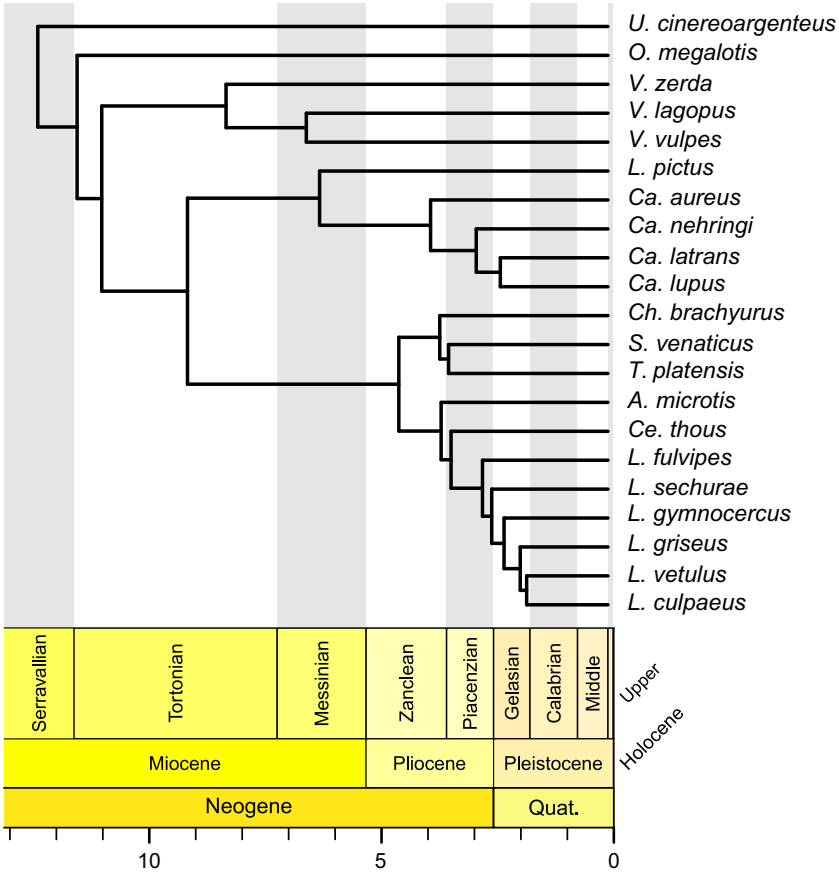

Fig. 1 Canid phylogeny after Zrzavý et al. (2018)

Bookstein (1991), and were placed on the mandibles to describe the variation of two mandibular modules: the ascending ramus and the alveolar region (Fig. 2, Table 1).

Data Analysis

To superimpose landmark configurations and to remove the spatial variation that does not correspond to shape, a generalized Procrustes analysis (GPA) was performed (Goodall 1991; Rohlf 1999). To visualize shape changes based on the position of the taxa in the morphospace and to identify the major components of variation, a Principal Components Analysis (PCA) was performed.

For comparative analyses, we produced a dataset containing a single configuration for each species. In the case that species had more than one individual, the mean shape for that species was used instead. The size was measured as the centroid size (square root of the squared distance between each landmark and the centroid of the unscaled configuration) and was also averaged for comparative analysis. Phylogenetic relationships among species were obtained from a recent comprehensive analysis including both extant and extinct species (Zrzavý et al. 2018).

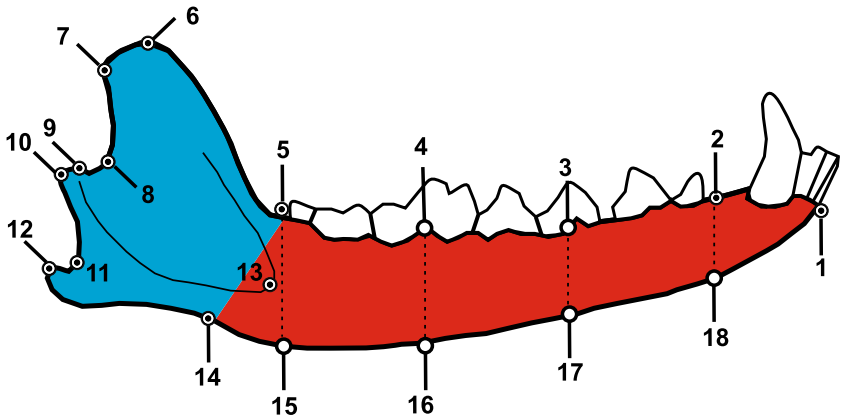

Fig. 2 Landmark configuration and partitions (blocks) on *Lycalopex gymnocercus* mandible. References: red, corpus mandibulae; blue, ramus mandibulae. Definitions in Table 1

Table 1 Mandibular landmarks, names and definitions used in the present study

Number	Name	Definition of landmarks
1	infradentale	alveoli dentalis of i1 on the midline.
2		projected point above of mandibular foramen.
3–4	semilandmarks	margo alveolaris of corpus mandibulae.
5		distal margin of the alveoli dentale of the last molar.
6		superiormost margin of the processus coronoideus.
7		distalmost margin of the processus coronoideus.
8		middle point in incisura mandibulae.
9	condylion medial	most medial margin of mandibular condyle.
10	condylion lateral	most lateral margin of mandibular condyle.
11		separation between collum mandibulae and processus angularis.
12		most dorsal-caudal tip of processus angularis.
13		anteriormost point of fossa masseterica.
14		point in the curved surface between corpus and ramus mandibulae.
15–18	semilandmarks	ventral border of corpus mandibulae.

Patterns of Evolution

We tested for the presence of significant evolutionary allometry on the sample by regressing shape variables on the log-transformed centroid size of the configurations using the phylogenetic Procrustes ANOVA implemented on the package Geomorph (Adams and Otárola-Castillo 2013). This method employs a permutation procedure (9999 permutations in the present case) to evaluate the significance of high-dimensional linear models while considering the phylogeny in a Generalized Least-Squares framework.

To infer the mode of shape evolution, we employed a Disparity Through Time (DTT) analysis of the Procrustes residuals. The DTT method is based on the calculation of the average within-clade disparity at each node on a dated phylogeny (Harmon et al. 2003). At the base of the phylogeny, the average disparity is at its maximum because the clade defined by that node encompasses all descendant species. As we advance in time, average disparities tend to decrease, as subclades encompass fewer species and morphological disparity, reaching the lower value (zero) at present. In the case of an "Early-Burst" scenario of diversification, we would expect to see an early decrease in average disparity at the beginning of the phylogeny, with later stabilization of average disparity, as different subclades are restricted within their own adaptive zones. Alternatively, if average disparities are constant throughout the history of the group, this could be associated with either a "Late-Burst" scenario or the presence of a stabilizing selection (single peak Ornstein-Uhlenbeck model). The empirical DTT curves were confronted against a null-distribution generated by simulating phenotypic evolution under a Brownian-Motion (BM) model (1000 simulations), and by calculating the Morphological Disparity Index (MDI) proposed by Slater et al. (2010). The MDI measures if the observed line falls above (positive values) or below (negative values) the expected by BM by quantifying the area between the empirical curve and the median of the simulated curves. The difference between the MDI of each simulated curve and the median was used as a null distribution of the BM model, and the empirical MDI was compared to it through a two-tailed test. Additionally, to interpret the DTT graphical results in terms of tempo of morphological evolution, we calculated graphical DTT intervals by employing the global envelope modification of the DTT analysis to control for multiple tests (Murrell 2018).

Furthermore, we also calculated the phylogenetic signal of mandible shape using the multivariate generalization of the K statistic, the K-mult (Adams 2014). This statistic measures how closely the pattern of phenotypic diversification resembles a BM model of evolution. If K-mult = 1 then morphological evolution matches exactly what is expected under BM. If K-mult<1, then distantly related relatives are closer to what would be expected under BM, suggesting convergent evolution or stabilizing selection. In the case that K-mult>1 species are thought to be more closely related to their sister taxa than what would be expected by BM.

Interspecific Integration

In order to evaluate the coordinated evolution of both mandibular modules (ascending ramus and the alveolar process), we employed a phylogenetic version of the Two-Block Least Squares approach. This approach consists of diagonalizing the between-block covariance matrix in order to extract the axis of phenotypic variation that explains the most between-block covariation (Rohlf and Corti 2000). We performed this analysis on the phylogenetic covariance matrix (Adams and Felice 2014) to take phylogenetic dependence into account.

For geometric morphometrics, this method is also called Singular Warp Analysis (Mitteroecker and Bookstein 2008) in which the eigenvectors of the between-block covariance matrix represent the axes of coordinated shape change of the whole landmark configuration. Because this analysis was performed on the phylogenetically informed covariance matrix, this analysis can be considered a phylogenetic Singular Warp Analysis (pSWA).

To evaluate if evolution happened along lines of most between-module integration, we performed a Principal Component Analysis (PCA) on the phylogenetic covariance matrix (Revell 2009). These phylogenetic principal components (pPCs) are the lines of most shape divergence after accounting for phylogenetic dependence (Polly et al. 2013). The first two pPCs were than compared to the first two pSW through vector correlation. High levels of vector correlation suggest that evolution happened along the lines of most between-block covariance and that integration was an important factor in the evolution of the canid mandible.

Integration between modules was measured as the covariance ratio (CR), which can be understood as the ratio of the overall covariation between modules relative to the overall covariation within modules (Adams 2016). As CR gets smaller (CR < 1), that means that within-module covariation is greater than between module covariation and that the structure is more modular. If values are larger (CR > 1) than between module covariation is larger than within-module covariation, suggesting that the structure is more integrated. The empirical CR value was confronted against 9999 values obtained through permutation of landmarks among modules. This test is devised to evaluate the null-hypothesis of no modularity, with the *p* value being estimated as the proportion of values that are smaller than the observed one.

Intraspecific Integration

To evaluate if macroevolutionary patterns were influenced by intraspecific constraints on shape variation, we first obtained pooled-within group covariance matrix for the following clades: *Urocyon* (*U. cinereoargenteus*, $n = 37$), *Vulpes* (*V. vulpes*, $n = 54$), *Canis* (*Ca. lupus*, $n = 6$), South American foxes (*Atelocynus microtis*, *Cerdocyon thous*, *Lycalopex culpaeus*, *L. griseus*, *L. gymnocercus*, *L. sechurae*, and *L. vetulus*, $n = 787$) and the "Aguará" clade (*Speothos venaticus* and *Chrysocyon brachyurus*, $n = 116$). As for interspecific data, we used the CR index as a measure of between-block integration. The use of CR is convenient in this case because the index is invariant to differences in sample sizes, and it is ideal to compare integration between different groups and scales (Adams 2016).

As for the intraspecific dataset, we calculated the axis of most-between module covariance through a SWA and the axis of most variance through PCA. SW1 obtained for the pooled data was then compared for the PC1 of the same dataset to evaluate if the main lines of phenotypic variation are aligned with the main lines of integration for intraspecific datasets. These calculations were performed for all clades, except for *Canis* due to insufficient sample size to adequately estimate both SW1 and PC1. Resulting SW1 and PC1 obtained for each within-group pooled covariance matrices were then compared among each other and with pSW1 and pPC1 through vector correlation. In the case that evolution was constrained by within-group patterns of variation and integration forming a LLR, we would expect a high alignment between axis obtained for the within-group samples and the ones obtained for the comparative datasets (Marroig and Cheverud 2010).

The visualization and graphics were made using the Morpho 2.6 R-package (Schlager 2017; R Core Team 2018) following Muñoz et al. (2017), which allows visualizing shape changes using color patterns.

Results

Patterns of Evolution

The phylogenetic regression of shape onto size was non-significant, explaining a very low portion of the shape change for the macroevolutionary data ($Df = 1$, $SS = 0.002$, $R2 = 0.054$, $F = 1.083$, $Z = 0.393$, $p = 0.335$). For this reason, we refrained from performing any size-correction in downstream analyses.

The DTT analysis revealed that average clade disparity is relatively constant throughout the history of the group (Fig. 3). Drops in average disparity are observed mainly at the base of the phylogeny with the divergence of Canini (sensu Zrzavý et al. 2018), which encompasses both South American canids and wolf-like groups (*Canis* and associated genera), and at more recent times, probably associated with within genera diversification of *Canis* and *Lycalopex*. After the initial drop, disparities are relatively constant, superseding what would be expected under drift. This result is mirrored by the MDI and phylogenetic signal analyses. While MDI showed a positive and significant value ($MDI = 0.198$, $p = 0.026$), the phylogenetic signal was low, despite being also significant ($K\text{-mult} = 0.568$, $p = 0.026$). While it might be possible that the observed pattern is due to incomplete species sampling, it is worth noticing that our sampling gaps are restricted to less inclusive taxa. Thus, while inclusion of more species probably might reveal details regarding patterns of evolution, our results are probably a good approximation of large-scale patterns for the group.

Interspecific Integration

The analysis of the evolutionary modularity of the mandible showed a high degree of between-module integration ($CR = 1.276$), which was larger than all values of the null hypothesis

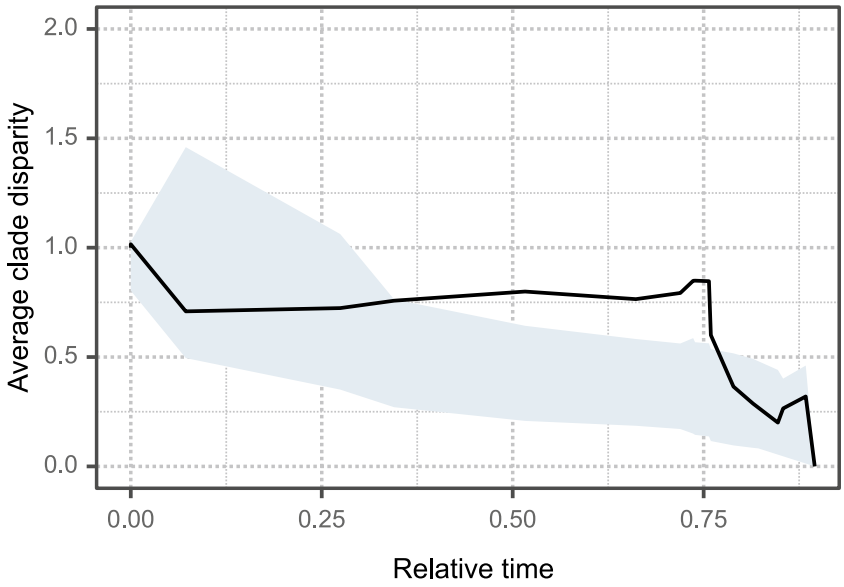

Fig. 3 Diversity through Time plot. Disparity is given in average clade disparity for Procrustes residuals. Both disparity and time are normalized by their maximum value, i.e., the maximum disparity and the height of the phylogeny, respectively. Black line represents the empirical disparity through time. Gray polygon represents the confidence interval corrected for multiple tests

of integration ($p = 1.000$). The phylogenetic PCA and SWA produced very similar results (Online Resource 1). In fact, the vector correlation between the first two sets of axes shows that they are almost collinear, with the correlation between pPC1 and pSW1 being 0.991 and the one between pPC2 and pSW2 being 0.956. Because the morphospace described by both analyses are so similar, we here focus on the space described by pSWA for simplicity.

The singular warp analysis shows that the first two pSWs explain more than 65% covariance among blocks (Fig. 4). The pSWs vectors can be visualized as colored surface deformations in Fig. 4. The shape changes associated with the pSW1 range from a slender mandible (around the average shape) to a robust-like mandible to more extreme positive values. Consequently, they show a robust mandible, a high alveolar ramus, the end of the tooth row closer to the fulcrum and a deep angular process, well-developed coronoid process, and an articular process closer to the occlusal plane. The pSW2 shape changes range from an elongated mandible with a very gracile alveolar ramus (negative values) to a short mandible with a deep and curved alveolar ramus (positive values). The morphospace depicted by these two pSWs clusters the omnivore forms around the origin, with the mesocarnivores and hypercarnivores towards positive values. The hypercarnivores show a larger disparity than omnivores and mesocarnivores forms, which can be accounted by the extreme position of *Ca. nehringi* towards positive values of pSW1 and *Speothos venaticus* and *Theriodictis platensis* in positive extreme and negative values of pSW2, respectively. While there is no clear phylogenetic pattern in the species dispersion along those axes, there seems to be a clear concentration of species around the average shape. As lineages diverge along the SW1 on the positive side, a subset of these also tends to diverge along SW2, both on positive or negative sides.

Intraspecific Integration

The CR index values calculated for the pooled within-group covariance matrices were considerably lower than the one observed for interspecific data (Fig. 5), ranging from 0.760 for *Vulpes* to 0.901 for *Urocyon*. All observed values were found to be lower than the majority of the null-distribution constructed by permuting points among modules ($p < 0.042$ for all analysis), suggesting that the within-group variation is modular in nature (see also Online Resource 2).

Vector correlation between PC1 and SW1 for each pooled within-group covariance matrix showed very low correlations, ranging from 0.004 to 0.091, suggesting that between-module integration is not aligned with the main directions of variation (Table 2). Despite this, the comparison of PC1 and SW1 among taxa showed high vector correlations (>0.6; see also Online Resource 3), suggesting that both lines of maximum variation and among module integration are conserved among canid species (Table 2).

While the comparison among the intraspecific PC1s and the pPC1 showed moderate correlation values, the comparison of intra-group SW1s with the evolutionary pSW1 shows the intraspecific vectors show small correlation with the interspecific one, contrary to what would expected if those lines where acting as LLR (Table 2).

Discussion

The mandible is a complex structure that can be shaped by diverse factors such as ontogeny, ecology, and evolutionary history (Prevosti et al. 2011). Here, we tried to parse these effects out by analyzing a large dataset of 3D morphometric data in a comparative approach. Our results show that

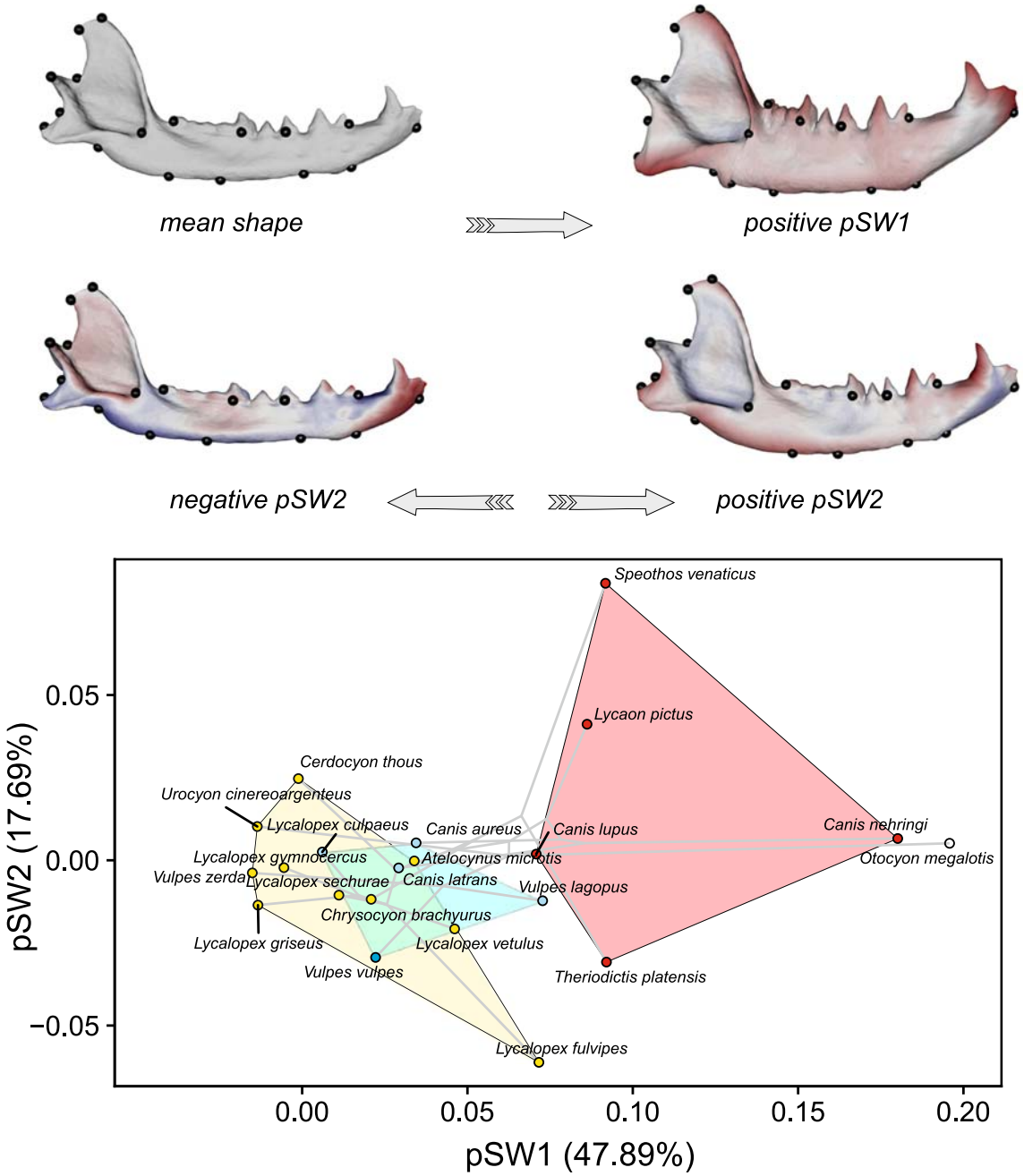

Fig. 4 Phylogenetic Singular Warp Analysis depicting the first two vectors of maximum covariation among modules. Dots represents species and gray lines represent the phylomorphospace reconstruction (Sidlauskas 2008) of the evolutionary trajectory. Gray mandible represents the mean shape. Colored mandibles are deformations from the mean shape to the extremes of the pSW axis. The minimum of pSW1 was omitted because it was similar to the mean shape

allometric scaling seems to have little influence in determining the mandibular shape of canids. This is in contrast with several studies that showed that allometry is one important factor affecting the shape in many other carnivoran lineages (Radinsky 1981a, 1981b, 1982; Segura et al. 2017) and in Canidae specifically (Wayne 1986; Penrose et al. 2016; Machado et al. 2018; Machado and Teta 2020). Because size has an effect on the whole organism, it has the capacity to integrate disparate parts of the organism, thus reducing modularity patterns and possibly hindering evolutionary outcomes (Mitteroecker and Bookstein 2007; Klingenberg 2009; Porto et al. 2013). For example, when allometric effects are strong, integration patterns (SW axes) and lines of most variance (PC axes) tend to converge (e.g., Sydney et al. 2012). Here, the comparison between intraspecific PC1s with SW1s shows that, within a taxa, those axes are

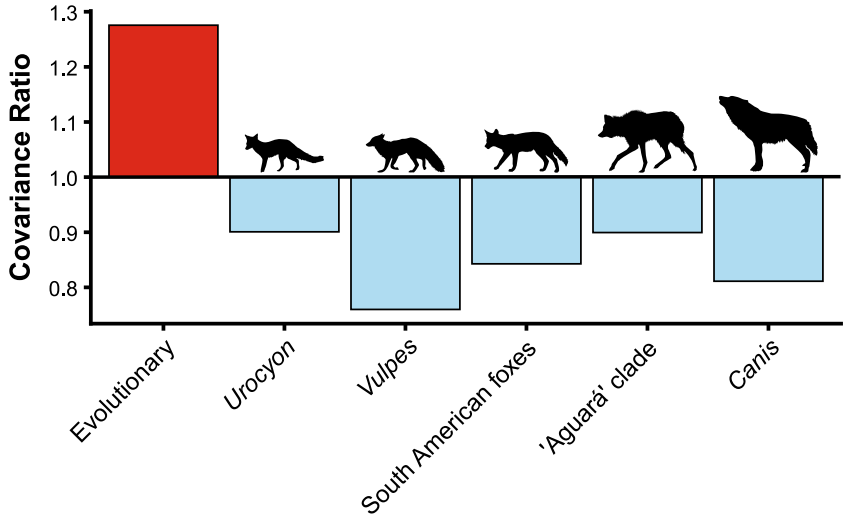

Fig. 5 Covariance Ratio (CR) indexes obtained for different matrices analyzed. Values that are significant under the permutation test are in blue and the ones that are not significant are in red. Values above 1 represent greater integration between modules and values below 1 represent a more modular structure

not the same. The lack of allometric scaling could then imply that the structure of the mandible is modular in nature, leading to higher evolvability of the structure (Hansen and Houle 2008).

However, while our intraspecific Covariance Ratios analyses showed that morphological variation in the mandible was modular on all accounts (as expected under weak allometric scaling), the comparative analysis failed to show any modularity (Fig. 5). This suggests that, despite being a modular structure in ontogenetic and genetic terms, the mandible is evolving as an integrated whole (see Oudot et al. 2019 for an example of the opposite pattern). The inspection of vector correlations are congruent with this conclusion: both intraspecific PC1s and SW1s were not aligned with evolutionary patterns depicted by pSW1 (Table 2). The lack of association between intraspecific axes of variation and evolutionary patterns further suggests a lack of a single LLR influencing the group (contra Conith et al. 2018). This suggests that, instead of being constrained by internal structural factors, the evolution of the mandible is more likely guided by functional demand (Greaves 1982, 1983; Rayner 1985).

The inspection of the between-species morphospace defined by the first phylogenetic Singular Warps (Fig. 4, or the identical phylogenetic Principal Component, Online Resource 1) shows a large lineage overlap (sensu Sidlauskas 2008) of species near the origin. This suggests that species were mostly evolving within a restricted region of the morphospace. Our Diversity Through Time analysis reinforces this idea, as average disparities were high throughout the evolutionary history of the group. Together with the presence of low phylogenetic signal, this pattern is consistent with a single-peak mode of evolution (Hansen 1997). In this model, the morphological disparity is restricted to a certain region of the morphospace, forcing lineages to revisit common regions repeatedly, eroding phylogenetic signal and erasing the effect of phylogenetic history on the determination of the phenotype. This could mean that the canid mandible presents a generalized shape that can be used by species with different diets and habits (see Silva et al. 2017 for a similar pattern). In fact, species clustered around the origin seem to be preferentially omnivorous and generalist in nature. These species are shown to possess mandibles that are slender (long and thin, see results) and to possess a shorter coronoid

Table 2 Vector correlation between PC1 and SW1 for each pooled within-group covariance matrix

	Axis type	Taxonomic scale	1	2	3	4	5	6	7	8
1	pSW1	Evolutionary								
2	SW1	*Urocyon*	0.262							
3	SW1	*Vulpes*	0.100	0.606						
4	SW1	South American foxes	0.256	0.864	0.800					
5	SW1	"Aguará" Clade	0.305	0.868	0.692	0.943				
6	PC1	*Urocyon*	0.573	0.075	0.033	0.084	0.079			
7	PC1	*Vulpes*	0.486	0.088	0.004	0.029	0.069	0.748		
8	PC1	South American foxes	0.553	0.020	0.049	0.041	0.019	0.910	0.918	
9	PC1	"Aguará" Clade	0.646	0.035	0.047	0.077	0.091	0.906	0.884	0.980

process, a combination that is thought to lead to lower killing bite forces (Radinsky 1981a, 1981b; Biknevicius and Ruff 1992; Christiansen 2008; Figueirido et al. 2010). While proportionally longer mandibles increase the shorter out lever arm, producing weaker bite forces, smaller coronoid processes also reduce the available area for muscle insertion. While a lower coronoid process might allow for a larger gape, which can be important during the killing bite, it is also tied to a decreased biting force (Greaves 1983; Christiansen 2008; Prevosti et al. 2011). Thus, species with this generalized morphology are probably better at quickly snatching smaller prey items, than they are at bringing down larger prey (Slater et al. 2009; Segura et al. in review).

Despite this apparent morphological constraint, some lineages can be seen as diverging from the common region in favor of more robust morphologies. Because these departures from the generalized morphology are associated with changes along the first pSW, they represent shape changes that are highly integrated throughout the structure (Fig. 4). This could have been achieved in two major ways. First, between-species changes could be aligned with lines of most integration among modules, as defined by the intraspecific covariation among mandibular regions. Our vector correlation analysis shows that is not the case, as pSW1 could not be considered to be aligned to the first SW obtained for any taxa. Alternatively, the association among traits can be achieved through functional demands, which force structures to change following specific rules in order to maintain functionality (Greaves 1982, 1983; Rayner 1985). This is probably the case for the mandible of Canidae, given that changes along with pSW1 form a gradient of shape variation that can be tentatively associated with diet in canids (see also Zurano et al. 2017).

According to our results, hypercarnivorous canids are shown to possess a more robust mandible (short, broad, and deep, see Results), which is an adequate morphology to undergo the stress of this type of diet (Biknevicius and Ruff 1992; Therrien 2005; Tseng and Binder 2009; Segura 2014). A shorter mandible implies a shorter out lever arm and, in consequence, a stronger bite force (Emerson and Radinsky 1980). Besides, the presence of well-developed coronoid, condylar, and angular processes produces larger areas of insertion for masticatory muscles, allowing for increased bite forces (Ewer 1998; Van Valkenburgh 1991). In this way, this configuration is associated with the biomechanical demands imposed by the necessity to bring down large prey and to better process and exploit vertebrate carcasses.

One clear exception for this pattern is the position of *Otocyon megalotis* among the hypercarnivorous morphs. This species is primarily insectivorous presenting a highly modified dentition that includes more molars than the rest of canids (Nowak 2005). The mandible of this species presents a bone structure called the subangular process or lobe located anteroventral to the angular process, on the region of the insertion of the digastric muscle (Ewer 1998). The digastric muscle inserts in the lobe and presents another line of action allowing for more rapid chewing, a feature that is used by the species to break down insect exoskeletons (Ewer 1998; Clark 2005). While the mandible of the species is somehow gracile, it does present a highly developed ascending ramus that is compatible with the one observed for hypercarnivorous forms. Furthermore, the presence of the subangular lobe makes the alveolar region relatively thicker than those of other foxes. These features might lead this species to "invade" the region restricted to hypercarnivores, as it converges with them in some features. Despite this, *O. megalotis* also differentiates from other species (hypercarnivores and omnivores alike) in the pSWs explaining lower levels of covariation (not shown). This suggests instead that the species is highly modified and does not fit the patterns observed for other species other than the obvious departure from the generalized omnivore morphology.

In summary, while the evolution of the mandible was mostly marked by the resampling of a restricted region of the morphospace, some divergence associated with ecology was observed, especially for highly specialized taxa (hypercarnivores and insectivores). Despite the fact that mandibles are modular in nature, conservation of function might have led to coordinated changes among modules, leading to an integrated evolution of both the ascending ramus and the alveolar region (Meloro et al. 2011). This evolution, however, did not follow a line of least resistance, and was marked mostly by stasis of shape. This contrasts to what is observed for the skull of Canidae, for which functional differences are described both at the intraspecific (Van Valkenburgh and Wayne 1994; Machado and Hingst-Zaher 2009; Segura 2014; Martinez et al. 2018; Schiaffini et al. 2019) and interspecific levels (Meloro et al. 2014; Bubadué et al. 2016; Zurano et al. 2017; Machado and Teta 2020; Machado in rev; Segura et al. in review). Direct comparisons between the evolution of mandible and skull shape in *Lycalopex culpaeus* shows that the mandible is less prone to change than the skull (Segura and Prevosti 2012; Segura 2014; Martinez et al. 2018), suggesting that morphological conservatism and adaptive change can be at play at the same time (Silva et al. 2017). Future work on diverse parts of the Canidae phenotype might be necessary to understand the interplay of different evolutionary forces shaping morphological disparity in the group.

Acknowledgments We thank to N. Toledo and S. Vizcaíno for inviting us to participate in this tribute to L.B. Radinsky within the framework of the Symposium: El paradigma de correlación forma-función en mastozoología: un tributo a Leonard Radinsky (1937–1985), which took place during the XXXI Jornadas Argentinas de Mastozoología, in La Rioja, Argentina, 25 October, 2018. For permission to access material under their care and the attention in mammal collections we thank Robert Voss, Eileen Westwig (AMNH), Sergio Bogan, Yolanda Davies (CFA), Rubén Barquez, Mónica Díaz (CML), Bruce Patterson (FMNH), Mauro Lucherini, Estela Luengos (GECM), Mauro Schiaffini, Gabriel Martin (LIEB), Andrés Pautasso (MFAZV), Pablo Teta, David Flores, Sergio

Lucero (MACN), Diego Verzi, Itatí Olivares (MLP), Mario de Vivo, Juliana Gualda (MZUSP), and Kristofer Helgen, Darrin Lunde (NMNH). This is a contribution to PICT 2014-1930, 2015-2389, 2015-0966, 2016-3151, 2016-3682, PUE 0125 and DEB 1350474 (NSF grant to Liam Revell).

Data Availability The datasets generated during and/or analyzed during the current study are available from the corresponding author on reasonable request.

Compliance with Ethical Standards

Conflict of Interest The authors declare that they have no conflict of interest.

Comment on Ethics This article does not contain any studies with human participants or animals performed by any of the authors.

Appendix 1. List of specimens used in this study

Atelocynus microtis (*N* = 23). AMNH: 76031; 76579; 95284; 95285; 98639; 100095. FMNH: 5249; 57836; 60674; 60675; 60676; 93955; 98080; 98081; 110949; 121286. MZUSP: 4320; 19750; 19751; 19752; 19753; 19754. NMNH: 361013.

Canis aureus (*N* = 1). MLP: 1035–1031.

Canis latrans (*N* = 1). MACN: 25.123.

Canis lupus (*N* = 5). AMNH: 18215. MACN 3.76; 23.15; 35.210. MLP: 1031.

Canis nehringi (*N* = 1). MACN-PV: 500.

Cerdocyon thous (*N* = 109). CFA: 3697; 3875; 4265; 4419; 4496; 4511; 4512; 4661; 4663; 4664; 4717; 5048; 5197; 5278; 5283; 5313; 5375; 6000; 6071; 6128; 6129. CML: 588; 3719; 3756; 3827; 4083; 4083; 4692; 5964; 5966; 5967; 6213; 6214; 6340. MACN: 4.213; 20.32; 24.85; 24.127; 25.119; 25.159; 29.839; 30.344; 30.345; 32.261; 32.262; 32.75; 33.6; 34.676; 36.191; 36.481; 39.460; 43.26; 44.11; 45.34; 45.40; 47.116; 47.189; 47.190; 47.191; 47.192; 47.193; 47.402; 48.3; 48.5; 48.6; 48.7; 48.10; 49.221; 49.367; 50.40; 50.43; 50.45; 50.57; 50.59; 50.60; 50.61; 50.62; 50.63; 50.64; 52.54; 52.63; 52.64; 13051; 14,322; 14681; 15741; 16189; 20316; 20454; 20456; 20815; 20816; 20817; 21228; 23180; 23669; 23670; 23726; 23727; 24045; 24046; 24207; 24208. MFA-ZV: 228; 1204. MLP: 20.IX.49.13; 16.X.01.7; 31.XII.02.77; 1322. MZUSP: 9687.

Chrysocyon brachyurus (*N* = 82). AMNH: 36962; 71179; 120999; 133940; 133941; 135274. CFA: 12826; 12827. CML: 1376; 6133; 6352. FMNH: 28311; 28312; 28313; 44534; 46003; 54406; 96003; 101848; 125401; 127434; 134483; 137425; 150739. MACN: 3.71; 3.73; 4.32; 4.303; 24.4; 30.29; 30.231; 53.49; 13466; 19146; 20646; 23456; 23984; 24043; 24201. MFA-ZV 517; 524; 581; 651; 652; 919; 1166. MLP: 2.IV.02.4; 5.X.99.1; 31.XII.02.88; 6; 92; 564; 695; 1684; 1686. MZUSP: 525; 3025; 3338; 9420; 19733; 19736; 29870; 31981; 32039; 32042; 32043; 32056; 32199; 32505; 32629. NMNH: 196975; 258614; 261022; 261023; 270371; 271567; 314863; 521007; 534807; 534970; 588,223; 588425.

Lycalopex culpaeus (*N* = 107). CFA: 2129; 6451. CML: 5067; 5068; 5069; 5070; 5071; 5970; 5974; 6343; 6344. LIEB: 791; 793. MACN: 3.68; 4.41; 7.42; 24.119; 25.128; 27.131; 30.69; 31.58; 31.59; 33.67; 33.68; 33.69; 38.39; 41.55; 15024; 15033; 15037; 15040; 15044; 15045; 15049; 15050; 15055; 15062; 15063; 15064; 15073; 15078; 15081; 15082; 15083; 15089; 15093; 15096; 15101; 15106; 15112; 15119; 15121; 15124; 15127; 15138; 15140; 15149; 15151; 15154; 15158; 15163; 15168; 15172; 15173; 15177; 15181; 15882; 15190; 15194; 15196; 15208; 15212; 15220; 15223; 15224; 15226; 15227; 15228; 15229; 15232; 15233; 15240; 15243; 15246; 15248; 19221; 19222; 20813; 21899; 23072; 23076; 23077; 23093; 23095; 23103; 23108; 23119; 23123; 23125; 23148; 23719; 23720; 23721; 23,915; 24210. MLP: 1264; 1266.

Lycalopex fulvipes (*N* = 2). FMNH: 23814; 23815.

Lycalopex griseus (*N* = 127). AMNH: 17440a; 17440b; 17441a. CFA: 2175; 4197; 5291; 5649; 5650; 5777; 5782; 10243. CML: 837; 838; 1177; 1178; 1427; 1489; 3714; 4967; 6189; 6190; 6192. FMNH: 154639; 154640. LIEB: 794; 809. MACN: 4.253; 23.20; 24.50; 24.52; 24.53; 24.54; 24.56; 24.57; 24.59; 24.62; 24.63; 24.64; 24.66; 24.68; 24.69; 24.71; 24.74; 24.75; 24.76; 24.79; 24.80; 24.81; 223; 225; 226; 13781; 14540; 14902; 15020; 15185; 15186; 15187; 15189; 15262; 15263; 15264; 15265; 15269; 16321; 16322; 16325; 20205; 20206; 20207; 20208; 20276; 20277; 20278; 20814; 20829; 23150; 23468; 23662; 23,663; 2664; 23668; 23718; 23728; 23729; 23730; 23910; 24206; 29.895; 50.419; 50.420; 50.432; 50.490; 51.170. MLP: 5.III.36.12; 5.III.36.27; 2.IV.60.1; 4.VIII.98.4; 240; 441; 559; 696; 701; 712. NMNH: 92139; 92140; 92141; 92142; 92143; 92144; 92145; 92146; 92147; 92149; 92150; 92151; 92152; 92169; 92173; 92174; 92175; 92176; 92177; 92178; 92179; 482163; 482164.

Lycalopex gymnocercus (*N* = 355). AMNH: 41502; 41503; 41504; 41505; 41506; 41507; 41508; 41509; 41510. CFA: 3255; 3698; 3962; 4256; 4406; 4416; 4417; 4659; 8312; 8313; 8588; 8589; 8590; 8591; 10887; 11062; 11063. CML: 192; 495; 545; 645; 834; 836; 895; 908; 909; 959; 1179; 1526; 1526; 3072; 4081; 4082; 5143; 5473; 5474; 5479; 5480; 5772; 6342. GECM: 24; 34; 40; 51; 57; 65; 67; 75; 76; 85; 100; 108; 112; 119; 121; 129; 139; 149; 152; 153; 179; 217Bis; 220Bis; 227Bis. MACN: 4.271; 20.33; 26.28; 20.35; 23.33; 23.34; 23.36; 23.37; 23.38; 24.48; 24.49; 24.133; 24.134; 24.140; 24.141; 24.142; 24.143; 24.144; 24.145; 24.146; 24.147; 24.148; 24.149; 24.151; 24.152; 24.154; 24.156; 24.162; 24.169; 24.170; 26.129; 26.162; 26.163; 27.53; 28.182; 29.35; 30.150; 30.210; 30.211; 30.212; 32.252; 32.263; 33.177; 33.266; 33.268; 34.317; 35.241; 36.178; 36.479; 36.480; 37.82; 38.243; 39.191; 39.194;

41.220; 41.221; 44.17; 48.266; 49.134; 49.139; 49.148; 49.149; 49.159; 49.160; 49.167; 50.56; 50.443; 50.491; 50.492; 50.494; 50.495; 50.497; 50.498; 50.500; 50.501; 50.502; 50.503; 50.504; 50.505; 51.81; 53.2; 54.133; 246; 285; 293; 13299; 13313; 13327; 13331; 13337; 14319; 14323; 14386; 14409; 15363; 15364; 15387; 15388; 15389; 15390; 15601; 15692; 15742; 15748; 15749; 15750; 15751; 15752; 15754; 15757; 15758; 15760; 15761; 15762; 15764; 15765; 1766; 157769; 15771; 15783; 15784; 15785; 15787; 15788; 15791; 15792; 15794; 15795; 15796; 15797; 15800; 15818; 15820; 15831; 15833; 15834; 15838; 15854; 15859; 15862; 15863; 15864; 15865; 15866; 15867; 15868; 15869; 15870; 15871; 15873; 15875; 15879; 15882; 15888; 15892; 15894; 15895; 15896; 15898; 15901; 15902; 15906; 15908; 15909; 15917; 15932; 15933; 15934; 15938; 15941; 15958; 15963; 15964; 15966; 15970; 15973; 15979; 15981; 15982; 15986; 15987; 15992; 15998; 15999; 16000; 16001; 16006; 16009; 16010; 16013; 16014; 16015; 16024; 16025; 16026; 16027; 16030; 16031; 16032; 16035; 16036; 16037; 16038; 16039; 16040; 16041; 16046; 16047; 16048; 16049; 16050; 16055; 16059; 16062; 16063; 16066; 16068; 16074; 16077; 16079; 16080; 16083; 16085; 16088; 16094; 16096; 16097; 16099; 16100; 16101; 16102; 16103; 16104; 16105; 16106; 16107; 16108; 16110; 16111; 16115; 16117; 16118; 16120; 16122; 16123; 16130; 16131; 16139; 16143; 16145; 16149; 16151; 22936; 23153; 23154; 23155; 23156; 23157; 23158; 23290; 23920; 24203; 24204; 24205; 24208; 24209; 24259; 24265; 24282. MLP: 16.III.99.16; 13.IV.99.3; 13.IV.99.13; 13.IV.99.14; 13.IV.99.36; 26.V.95.9; 4.VIII.98.9; 30.XII.02.65; 710. NMNH: 172789; 172790; 236366; 331065.

Lycalopex sechurae ($N = 35$). AMNH: 100091; 100100; 133926; 133927; 133928; 133929; 133937; 2091; 349; 36457; 391; 46525; 46526; 46527; 46528; 46529; 46530; 46531; 46532; 46533; 63709; 70091. FMNH: 19971; 19972; 20747; 53911; 80953; 80954; 80955; 80956; 80957; 80958; 80959; 80960; 80961; 80962; 80963; 80964; 80965; 80966; 80967; 80968; 80969.

Lycalopex vetulus ($N = 31$). MLP: 1258. MZUSP: 1011; 1012; 1014; 1015; 1016; 1018; 1075; 1076; 1084; 12040; 13611; 3046; 3047; 3047; 3048; 3049; 3050; 825. NMNH 121171; 121172; 181150; 545109.

Speothos venaticus ($N = 34$). AMNH: 136285; 167846; 175306; 184688; 37472; 76035; 76805; 76806; 98558; 98559; 98560; 98640. FMNH: 121544; 125402; 60290; 87861. MACN: 50.67; 16510. MZUSP:19743; 19744. NMNH: 253504; 270165; 270171; 270368; 270369; 270370; 307650; 314048; 395841; 398030; 521045; 538307; 544414; 582465.

Urocyon cinereoargenteus ($N = 37$). AMNH: 255645; 255648; 254470; 8197; 243449; 100301; 243095; 120989; 184105; 184122; 184012; 183939; 184002; 184065; 183979; 184098; 184094; 184077; 184091; 184126; 184083; 184121; 184014; 184087; 184013; 184009; 183991; 183956; 183942; 183943; 183960; 183953; 183995; 183954; 185512; 184064; 184007.

Vulpes lagopus ($N = 1$). MACN: 4.1.

Vulpes vulpes ($N = 54$). FMNH: 106726; 107271; 140172; 140176; 74472; 74987; 74988; 74989; 75644; 75645; 75646; 77130; 77136; 78650; 78651; 80827; 80829; 80836; 80837; 80839; 80840; 84697; 84698; 85216; 85217; 85218; 86820; 89369; 89370; 89371; 89372; 89587; 89710; 89712; 89963; 90361; 90473; 90474; 91605; 91725; 91726; 91731; 91741; 92727; 95863; 95865; 95867; 95870; 95872; 95873; 98733; 98734; 98735; 98736.

Vulpes zerda ($N = 2$). CML: 3731. MACN: 3.14.

Theriodictis platensis ($N = 1$). MLP-PV: 96-IX-1-1.

Otocyon megalotis ($N = 1$). MACN: 26.115.

Lycaon pictus ($N = 1$). MACN: 38.249.

References

Adams DC (2014) A generalized K statistic for estimating phylogenetic signal from shape and other high-dimensional multivariate data. Syst Biol 63:685–697

Adams DC (2016) Evaluating modularity in morphometric data: challenges with the RV coefficient and a new test measure. Methods Ecol Evol 7:565–572. https://doi.org/10.1111/2041-210X.12511

Adams DC, Felice RN (2014) Assessing trait covariation and morphological integration on phylogenies using evolutionary covariance matrices. PLoS One 9:e94335–e94338

Adams DC, Otárola-Castillo E (2013) Geomorph: an R package for the collection and analysis of geometric morphometric shape data. Methods Ecol Evol 4:393–399

Biknevicius AR, Ruff CB (1992) Use of biplanar radiographs for estimating cross-sectional geometric properties of mandibles. Anat Rec 232:157–163

Bookstein FL (1991) Morphometric Tools for Landmark Data. Geometry and Biology. Cambridge University Press, New York

Bubadué J de M, Cáceres N, Santos Carvalho R dos, Meloro C (2016) Ecogeographical variation in skull shape of South-American canids: abiotic or biotic processes? Evol Biol 43: 145–159

Cerny R, Lwigale P, Ericsson R, Meulemans D, Epperlein H. H, Bronner-Fraser M (2004) Developmental origins and evolution of jaws: new interpretation of "maxillary" and "mandibular." Dev Biol 276:225–236

Cheverud JM (1996) Developmental integration and the evolution of pleiotropy. Am Zool 36:44–50

Christiansen P (2008) Evolution of skull and mandible shape in cats (Carnivora: Felidae). PLoS One 3:e2807

Clark HO (2005) *Otocyon megalotis*. Mammal Species 766:1–5

Conith AJ, Meagher MA, Dumont ER (2018) The influence of climatic variability on morphological integration, evolutionary rates, and disparity in the Carnivora. Am Nat 191:704–715

Curth S, Fischer MS, Kupczik K (2017) Patterns of integration in the canine skull: an inside view into the relationship of the skull modules of domestic dogs and wolves. Zoology 125:1–9

Echarri S, Prevosti FJ (2015) Differences in mandibular disparity between extant and extinct species of metatherian and placental carnivore clades. Lethaia 48:196–204

Emerson SB, Radinsky LB (1980) Functional analysis of sabretooth cranial morphology. Paleobiology 6:295–312

Esteve-Altava B (2017) In search of morphological modules: a systematic review. Biol Rev 92:1332–1347

Ewer RF (1998) The Carnivores. Cornell University Press, Ithaca

Figueirido B, Serrano-Alarcón FJ, Slater GJ, Palmqvist P (2010) Shape at the cross-roads: homoplasy and history in the evolution of the carnivoran skull towards herbivory. J Evol Biol 23:2579–2594

Garcia GRG, Hingst-Zaher E, Cerqueira R, Marroig G (2014) Quantitative genetics and modularity in cranial and mandibular morphology of *Calomys expulsus*. Evol Biol 41:619–636. doi: https://doi.org/10.1007/s11692-014-9293-4

Goodall CR (1991) Procrustes methods in the statistical analysis of shape. J Roy Stat Soc Ser B (Methodological) 53:285–339

Greaves WS (1982) A mechanical limitation on the position of the jaw muscles of mammals: the one-third rule. J Mammal 63:261–266

Greaves WS (1983) A functional analysis of carnassial biting. Biol J Linnean Soc 20:353–363

Hallgrímsson B, Jamniczky H, Young NM, Rolian C, Parsons TE, Boughner JC, Marcucio RS (2009) Deciphering the palimpsest: studying the relationship between morphological integration and phenotypic covariation. Evol Biol 36:355–376

Hansen T (1997) Stabilizing selection and the comparative analysis of adaptation. Evolution 51:1341–1351

Hansen T, Houle D (2008) Measuring and comparing evolvability and constraint in multivariate characters. J Evol Biol 21:1201–1219

Harmon LJ, Schulte JA, Larson A, Losos JB (2003) Tempo and mode of evolutionary radiation in iguanian lizards. Science 301:961–964

Holliday JA, Steppan SJ (2004) Evolution of hypercarnivory: the effect of specialization on morphological and taxonomic diversity. Paleobiology 30:108–128

Klingenberg CP (2008) Morphological integration and developmental modularity. Annu Rev Ecol Evol Syst 39:115–132

Klingenberg CP (2009) Morphometric integration and modularity in configurations of landmarks: tools for evaluating a priori hypotheses. Evol Dev 11:405–421

Klingenberg CP, Leamy LJ, Cheverud JM (2004) Integration and modularity of quantitative trait locus effects on geometric shape in the mouse mandible. Genetics 166:1909–1921

La Croix S, Holekamp KE, Shivik JA, Lundrigan BL, Zelditch ML (2011a) Ontogenetic relationships between cranium and mandible in coyotes and hyenas. J Morphol 272:662–674

La Croix S, Zelditch ML, Shivik JA, Lundrigan BL, Holekamp KE (2011b) Ontogeny of feeding performance and biomechanics in coyotes. J Zool 285:301–315

Larouche O, Zelditch ML, Cloutier R (2018) Modularity promotes morphological divergence in ray-finned fishes. Sci Rep 8:7278

Machado FA, Hingst-Zaher E (2009) Investigating South American biogeographic history using patterns of skull shape variation on *Cerdocyon thous* (Mammalia: Canidae). Biol J Linnean Soc 98: 77–84

Machado FA, Teta P (2020) Morphometric analysis of skull shape reveals unprecedented diversity of African Canidae. J Mammal

Machado FA, Zahn TMG, Marroig G (2018) Evolution of morphological integration in the skull of Carnivora (Mammalia): changes in Canidae lead to increased evolutionary potential of facial traits. Evolution 72:1399–1419

Marroig G, Cheverud JM (2010) Size as a line of least resistance II: direct selection on size or correlated response due to constraints? Evolution 64:1470–1488

Martinez PA, Pia MV, Bahechar IA, Molina WF, Bidau CJ, Montoya-Burgos JI (2018) The contribution of neutral evolution and adaptive processes in driving phenotypic divergence in a model mammalian species, the Andean fox *Lycalopex culpaeus*. J Biogeogr 3:595–512

Meloro C, Hudson A, Rook L (2014) Feeding habits of extant and fossil canids as determined by their skull geometry. J Zool 295:178–188

Meloro C, O'Higgins P (2011) Ecological adaptations of mandibular form in fissiped Carnivora. J Mammal Evol 18:185–200

Meloro C, Raia P, Carotenuto F, Cobb SN (2011) Phylogenetic signal, function and integration in the subunits of the carnivoran mandible. Evol Biol 38:465–475

Meloro C, Raia P, Piras P, Barbera C, O'Higgins P (2008) The shape of the mandibular corpus in large fissiped carnivores: allometry, function and phylogeny. Zool J Linn Soc 154:832–845

Mitteroecker P, Bookstein FL (2007) The conceptual and statistical relationship between modularity and morphological integration. Syst Zool 56:818

Mitteroecker P, Bookstein F (2008) The evolutionary role of modularity and integration in the hominoid cranium. Evolution 62:943–958

Muñoz NA, Cassini GH, Candela AM, Vizcaíno SF (2017) Ulnar articular surface 3-D landmarks and ecomorphology of small mammals: a case study of two early Miocene typotheres (Notoungulata) from Patagonia. Earth Env Sci Trans R Soc 106:315–323

Murrell DJ (2018) A global envelope test to detect non-random bursts of trait evolution. Methods Ecol Evol 9:1739–1748

Nowak RM (2005) Walker's Carnivores of the World. John Hopkins University Press, London

Olson EC, Miller RL (1958) Morphological Integration. University of Chicago Press, Chicago

Oudot M, Neige P, Laffont R, Navarro N, Khaldi AY, Crônier C (2019) Functional integration for enrolment constrains evolutionary variation of phacopid trilobites despite developmental modularity. Palaeontology 4:393–317. https://doi.org/10.1111/pala.12428

Parr WC, Wilson LA, Wroe S, Colman NJ, Crowther MS, Letnic M (2016) Cranial shape and the modularity of hybridization in dingoes and dogs; hybridization does not spell the end for native morphology. Evol Biol 43:171–187.

Penrose F, Kemp GJ, Jeffery N (2016) Scaling and accommodation of jaw adductor muscles in Canidae. Anat Rec 299:951–966

Polly PD, Lawing AM, Fabre AC, Goswami A (2013) Phylogenetic principal components analysis and geometric morphometrics. Hystrix 24:33–41

Porto A, Shirai LT, Oliveira FB, Marroig G (2013) Size variation, growth strategies, and the evolution of modularity in the mammalian skull. Evolution 67:3305–3322. https://doi.org/10.1111/evo.12177

Prevosti FJ, Turazzini GF, Ercoli MD, Hingst-Zaher E (2011) Mandible shape in marsupial and placental carnivorous mammals: a morphological comparative study using geometric morphometrics. Zool J Linn Soc 164:836–855

Prevosti FJ, Segura V, Cassini GH (2013) Revision of the systematic status of Patagonian and Pampean gray foxes (Canidae: *Lycalopex griseus* and *L. gymnocercus*) using 3D geometric morphometrics. Mastozool Neotrop 20:289–300

R Core Team (2018) R: A Language and Environment for Statistical Computing. R Foundation for Statistical Computing, Vienna

Radinsky LB (1981a) Evolution of skull shape in carnivores 1. Representative modern carnivores. Biol J Linnean Soc 15:369–388

Radinsky LB (1981b) Evolution of skull shape in carnivores 2. Additional modern carnivores. Biol J Linnean Soc 16:337–355

Radinsky LB (1982) Evolution of skull shape in carnivores. 3. The origin and early radiation of the modern carnivore families. Paleobiology 8:177–195

Rayner JM (1985) Linear relations in biomechanics: the statistics of scaling functions. J Zool 206:415–439

Revell LJ (2009) Size-correction and principal components for interspecific comparative studies. Evolution 63:3258–3268

Rohlf FJ (1999) Shape statistics: Procrustes superimpositions and tangent spaces. J Classif 16:197–223

Rohlf FJ, Corti M (2000) Use of two-block partial least-squares to study covariation in shape. Syst Zool 49:740

Schiaffini MI, Segura V, Prevosti FJ (2019) Geographic variation in skull shape and size of the pampas fox *Lycalopex gymnocercus* (Carnivora: Canidae) in Argentina. Mammal Biol 97:50–58

Schlager S (2017) Morpho and Rvcg - shape analysis in R. In: Zheng G, Li S, Szekely G (eds) Statistical Shape and Deformation Analysis. Academic Press, London, pp 217–256

Schluter D (1996) Adaptive radiation along genetic lines of least resistance. Evolution 50:1766–1774

Segura V (2014) Ontogenia craneana postnatal en canidos y felidos neotropicales: funcionalidad y patrones evolutivos. Ph.D. Thesis, Universidad Nacional de La Plata, Argentina

Segura V, Cassini GH, Prevosti FJ (2017) Three-dimensional cranial ontogeny in pantherines (*Panthera leo*, *P. onca*, *P. pardus*, *P. tigris*; Carnivora: Felidae). Biol J Linnean Soc 120:210–227

Segura V, Prevosti FJ (2012) A quantitative approach to the cranial ontogeny of *Lycalopex culpaeus* (Carnivora: Canidae). Zoomorphology 131:79–92

Sidlauskas B (2008) Continuous and arrested morphological diversification in sister clades of characiform fishes: a phylomorphospace approach. Evolution 62:3135–3156

Silva FM, Prudente ALDC, Machado FA, Santos MM, Zaher H, Hingst-Zaher E (2017) Aquatic adaptations in a Neotropical coral snake: a study of morphological convergence. J Zool Syst Evol Res 4:393–313. https://doi.org/10.1111/jzs.12202

Slater GJ, Dumont ER, Van Valkenburgh B (2009) Implications of predatory specialization for cranial form and function in canids. J Zool 278:181–188. https://doi.org/10.1111/j.1469-7998.2009.00567.x

Slater GJ, Price SA, Santini F, Alfaro ME (2010) Diversity versus disparity and the radiation of modern cetaceans. Proc R Soc B-Biol Sci 277:3097–3104

Sydney NV, Machado FA, Hingst-Zaher E. (2012) Timing of ontogenetic changes of two cranial regions in *Sotalia guianensis* (Delphinidae). Mammal Biol 77:397–403

Therrien F (2005) Mandibular force profiles of extant carnivorans and implications for the feeding behaviour of extinct predators. J Zool 267:249–270

Tseng ZJ, Binder WJ (2009) Mandibular biomechanics of *Crocuta crocuta*, *Canis lupus*, and the late Miocene *Dinocrocuta gigantea* (Carnivora, Mammalia). Zool J Linnean Soc 158:683–696

Van Valkenburgh B (1991) Iterative evolution of hypercarnivory in canids (Mammalia: Carnivora): evolutionary interactions among sympatric predators. Paleobiology 17:340–362

Van Valkenburgh B, Wayne RK (1994) Shape divergence associated with size convergence in sympatric East African jackals. Ecology 75: 1567–1581

Wainwright PC, Reilly SM (1994) Ecological Morphology. University of Chicago Press, Chicago

Wayne RK (1986) Cranial morphology of domestic and wild canids: the influence of development on morphological change. Evolution 40 (2):243–261

Zrzavý J, Duda P, Robovský J, Okřinová I, Řičánková VP (2018) Phylogeny of the Caninae (Carnivora): combining morphology, behaviour, genes and fossils. Zool Scr 47:373–389

Zurano JP, Martinez PA, Canto-Hernandez J, Montoya-Burgos JI, Costa GC (2017) Morphological and ecological divergence in South American canids. J Biogeogr 44:821–833